Qatar Univ. Sci. J. (1996), 16(1): 61-68

SOLID-STATE AC-CONDUCTIVITY ANALYSIS FOR THE LONG DEBATED CATALYTIC ACTIVITY OF THE BORALITE SIEVE

By

MOEIN B. SAYED
Chemistry Department, Faculty of Science, Qatar University, Doha, P. O. Box 2713, Qatar

تحليل كهربي لانخفاض كفاءة حفز خام البوراليت عن مثيله زيوليت HZSM-5

عبد المعين بركات سيد

تم في هذا البحث عمل دراسه مقارنة لكفاءة التوصيل الكهربي (كداله كفاءة الحفز) لخام البوراليت المشتق من زيوليت HZSM-5 باحلال تام لعنصر الالومنيوم بالبورون الأكثر حمضية في شبكة الالومينيوسيليكات البلوريه والمتوقع له أن يزيد من كفاءة الحفز . توضح النتائج أهمية دور الماء (المدمص في مسام الخام) دون درجة الغليان ، حيث تنخفض درجة التوصيل مع الحراره لتصل أدنى معدل عند درجة 373 K . ترتفع درجة التوصيل عقب ذلك ولكن من خلال ميكانيكيه أخرى تعتمد على التوصيل البروتوني الذي يميز البوراليت بكفاءة توصيل تماثل عشرة أضعاف HZSM-5 من خلال جمله مفارقات . مثلا بالمقارنه لارتفاع درجة التوصيل المنتظم مع ارتفاع درجة الحرارة ، جرعة التعرض لأشعة جاما وتردد التيار الكهربي تنخفض درجة توصيل البوراليت عند التعرض لظروف قاسية من تلك العوامل . أمكن تفسير ذلك في ضوء اختلاف حمضية بروتونات البوراليت المعادله لعنصر البـورون عنهـا في HZSM-5 المعادله لعنصر الالومينيوم . بالمقارنة لتجانس واستقرار بروتونات الزيوليت تختلف بروتونات البوراليت حيث تنخفض درجة استقرار بروتونات البوراليت الأكثر حمضية . نظراً لضرورة معالجة الخام عند درجة حرارة مرتفعة لتنشيط كفاءة الحفز وكذلك ارتفاع حرارة تفاعلات الحفز يغيب دور بروتونات البوراليت شديدة الحمضية والتي تميزه بدرجة توصيل كهربي وكفاءة حفز عاليه عند درجات الحرارة المنخفضة ، وهكذا يبدو خام البوراليت قليل الكفاءة عند درجات حرارة الحفز العالية ، على غير المتوقع .

Key Words: Ac-conductivity, Boralite, HZSM-5

ABSTRACT

The ac-phase dependent impedance, capacitance and dielectric loss of boralite are measured and correlated with those of a similar history HZSM-5 as a function of frequency (0.1-100 kHz) and temperature (373-638 K) at 0.8 V. The data illustrate distorted semicircle impedance Z"(Z') and linear permittivity ε"(ε') dependences throughout the temperature range. Below 373 K, the conduction is assisted by sorbed water, as its role diminishes with desorption and vanishes above 373 K. Thermally activated protonic conduction becomes more dominant at higher temperatures. Compared to the steady conduction in HZSM-5, the boralite permittivity reveals a conduction shifting across 573 K in

temperature controlled regimes. Below 573 K the conduction is characterized by low activation energy of 0.09±0.01 eV, compared to the higher temperature conduction of the energy 0.37 eV. The latter conduction is sensitive to variation in the field frequency and irradiation dose of gamma rays. For instance, the 0.37 eV activation energy measured at 0.1 kHz falls to 0.19 eV if measured at 100 kHz and to 0.13 eV if exposed to 10 Mrad gamma dose. Such energy losses can be assigned to rises in the mobility of the conduction Bronsted sites. Compared to the steady rise in HZSM-5 conductivity, irradiation at higher doses reduces the boralite conductivity. This latter result suggests that the B-associated Bronsted sites are heterogeneous; the more mobile site is of so low stability that it cannot sustain the impact of integrated heat, irradiation and field frequency. They might undergo dehydroxylation or trapping as lattice defects under the impact of such reinforcing parameters. The apparently low activity of boralite can then be addressed to the low stability of its highly mobile B-associated Bronsted sites. Silicalite shows incomparable low conductivity that supports the more important role of the charge carriers, Bronsted sites in the conduction in both the boralite and HZSM-5 sieves.

INTRODUCTION

For modifying the catalytic features of zeolites, attempts of isomorphously replacing the lattice silicon Si and/or aluminium Al with relevant elements viz. Ge, B, Ga, Cr, Fe, V, Ti, Ce, Zr or P have been conducted [1-5].On the basis of the more active chemistry of B over Al, it was conceived that replacing the former for the latter element in zeolites would enhance the catalytic activity. Also, because of its smaller atom, incorporation of B in the lattice would reduce the unit cell volume into a more selective zeolite. This approach has been followed for modifying the catalytic features of HZSM-5, the famous zeolitic catalyst of Mobil applied to the conversion of methanol into gasoline [6]. A considerable number of patents and papers [7-9] have witnessed the birth of boralite, a new ZSM-5-like [10,11] sieve. In this sieve, B occupies a similar site [12-15] to the zeolite Al. The resultant B-associated sites should, therefore, characterize the new sieve with Bronsted as well as Lewis acidities. Few reports [16-18] have claimed activity for boralite in processes catalyzed by Bronsted acidity. Such B-associated Bronsted sites have been reported [19-22] to absorb ir radiation at 3695 cm^{-1} that being considered as a mid frequency,compared to the Al-associated Bronsted sites at 3610 cm^{-1} and the surface silanols at 3730 cm^{-1}. Since band frequency is associated with the oscillating bond order,B-associated Bronsted sites are then regarded as moderately acidic [22-24]. Nevertheless, a tailing band appearing at the lower frequency side of the 3695 cm^{-1} band may disclose incorporation of a range of heterogeneously distributed Bronsted sites of higher acidity and lower thermal stability.

The aim of this work is to report on the ac-conductivity of the microporous sieve, boralite, with reference to the recently reported [25] HZSM-5 and B-modified HZSM-5 [26] of typical structure and similar history, hoping to reach a probable answer for the apparent low activity of the boralite sieve debated for a long time.

EXPERIMENTAL

MATERIALS

Following the procedure reported in the French patents [27,28], the boralite molecular sieve was prepared from pure SiO_2 and H_3BO_3, using NH_4F as a medium and TPABr as a template, at pH of nearly 7 in a teflon vessel-contained autoclave. The resultant NH_4,TPA-form was then gently decomposed under a stream of dry N_2 at 623 K into the H-form that shows a unit cell composition of $H_{3.45}B_{3.43}Al_{0.02}Si_{92.55}O_{192}$. The calcined boralite sample shows high crystallinity, which was evident [13,29,30] by the vibrational band absorbance (560/455 cm^{-1}) ratio of 0.62 and quite sharp and intense X-ray powder diffraction. The boralite sample was correlated in the present study with a well identified HZSM-5 sample formed by also gentle decomposition of the NH_4-form and characterized by almost similar crystallinity (30x12x8 μm particle size compared to 50x25x20 μm of boralite) and comparable unit cell composition of $H_{3.6}K_{0.5}Al_{4.1}Si_{91.9}O_{192}$. However, a number of remarkable features still distinguish the two sieves. Most important is boralite shows rather short term activity for the hydrocarbon formation and reactions, compared with the pronounced long term activity of HZSM-5. Nevertheless,boralite shows higher activity in other reactions catalysed at lower temperatures, e.g. the methanol dehydration into ether. Boralite shows ir spectrum distinguished by a band at 920 cm^{-1} assigned to the Bi-O-Si out-of-plane deformation and by asymmetric band at 3695 cm^{-1} assigned to B-associated Bronsted site stretching mode,compared to the more symmetric Al-associated Bronsted band at 3610 cm^{-1} of HZSM-5. The present boralite shows a reduction by 110 A^{o3} in the unit cell volume (5375 A^{o3}) of HZSM-5 into a unit cell volume of 5265 A^{o3} that effected loss (7.4 to 6.4 wt%) by 14% in the 3-Me-pentane sorption capacity. Such a sorption loss is much higher than that accounted by the loss (about 2%) in the unit cell volume. The sorption loss must therefore be a consequence of constraint, since the sorption capacity of n-hexane was found as 11 wt% for both the sieves. The loss in bond length effected by replacing B-O (1.39 A^o) for Al-O (1.67 A^o) is 17%.Since the replacement is only 84%,the overall loss in the constraining factor (17% x 0.84) is only 14% as is experimentally found by 3-Me-pentane sorption.Extra lattice boron is improbable as this boralite obeys the linear dependence of unit cell volume on the zeolite boron content.Hence,contribution of such lattice defects is believed minor. Similar history of the two molecular sieves would help in appropriately identifying origin of the long debated low activity of boralite, with respect to HZSM-5.

METHODS AND EQUIPMENT

Several batches of the boralite sieve were gamma-irradiated at different doses at 300 K, using a ^{60}Co gamma cell 220, manufactured by Atomic Energy of Canada Ltd. The 10 and 100 Mrad irradiated batches were selected, together with fresh boralite, HZSM-5 and silicalite samples for the discussion. These materials were sampled as 0.1 cm thick disks suitable for the ac-conductivity measurements. The disks were treated as shown elsewhere [25]. Each disk was tightly interfaced with two silver polished disks of the area 1.33 cm^2. The latter disks were sandwiched between the copper electrodes of the type used previously [25]. The measurements were performed at 0.1-100 kHz, 373-638 K and 0.8 V, using a Hioki 3520 LCR tester for analysis of the frequency-dependent impedance Z^*, capacitance C^* and dielectric loss tan δ of the samples. Infrared spectra in the O-H stretching region of 4000-3000 cm^{-1} were measured for self-supporting wafers pretreated at 10^6 torr and 673 K. The spectra at more mild pretreatment conditions are less informative because of contribution of the strongly H-bonded Bronsted sites and other surface silanols. For this reason the effect of gamma irradiation on the mobility of such species could unfortunately not be spectrally probed, as gamma is known to lose its structural induced effects at such elevated temperatures of ≥ 673 K.

TECHNIQUE

It might be helpful to present a brief introduction of the technique so that its advantages over other more conventional techniques of zeolite characterization can be appreciated. Among the long range electrical features, the electric impedance and capacitance are of interest as they help in qualitatively identifying the mode of conduction and quantitatively determining the conductivity. Characterization of the zeolite acidity and activity can advantageously be performed in a temperature range inaccessible to other techniques inevitably necessitate high pretreatment temperatures. The electric conductivity associates with the number and mobility of the conduction charge carriers. In protonic zeolites and based on the established postulates of Arrhenius, the electric conductivity is considered as an appropriate measure for the zeolite acidity and activity features.

A brief theoretical consideration can be put forward as follows:

The LCR tester measures the electric impedance and capacitance as complex figures that combine in phase **Z'** or **C'** and out-of-phase **Z"** or **C"** terms distinguished by the **cos** and **sin** functions of the phase angle θ and by the term $\mathbf{j = -1^{1/2}}$ as follows:

$$Z^* = Z' - jZ'' \qquad\qquad C^* = C' - jC''$$

$$= Z^*\cos\theta - jZ^*\sin\theta \qquad\qquad = C^*\sin\theta - jC^*\cos\theta$$

in phase out-of-phase   **in phase out-of-phase**

The current I passing through a resistor R under the applied field E is given by Ohm's law:

$$I = E/R \qquad (1)$$

A pure capacitor allows a frequency dependent ac-current:

$$I = jWC^*E \qquad (2)$$

where W is the angular frequency 2πf

The impedance of the capacitor ($Z^* = R = 1/jWC^*$) is imaginary (eqns 1,2) since it contains the term **j**. This indicates difference in the phase angle of 90° between the sinusoidal current and voltage that shared by the angles **θ** and **δ.**

In circuits containing **R** and **C** in series, the complex impedance Z^* is given as

$$Z^* = R + 1/jWC^*$$
$$= R - j/WC^* \qquad (3)$$
$$= Z' - jZ''$$

$$Z' = R \qquad Z'' = 1/WC^* \qquad (4)$$

For circuits containing **R** and **C** in parallel, the admittance A^* is given as:

$$A^* = 1/Z^* = 1/R + jWC^* \qquad (5)$$

The complex admittance A^* separates into real **A'** and imaginary **A"** components:

$$A^* = A' + jA'' \qquad (6)$$

$$A' = 1/R \qquad A'' = WC^* \qquad (7)$$

$$Z^* = A^{*-1} = R/1+jWRC^* \qquad (8)$$

multiply by the conversion factor $\mathbf{1-jWRC^*}$

$$Z^* = R/1+(WRC^*)^2 - jWR^2C^*/1+(WRC^*)^2 \qquad (9)$$

Therefore,

$$Z' = R/1+(WRC^*)^2 \text{ and } Z'' = WR^2C^*/1+(WRC^*)^2$$

Plotting the complex **Z"(Z')** dependence is useful for calculating the dc-resistance R_o and hence dc-conductivity as the plot shows that $Z' = R_o$ when **Z"** tends to zero.

For a solid electrolyte, the equivalent circuit is a combination of resistance R_b and capacitance C_b in parallel for the bulk electrolyte, along with capacitance C_{gb} in series for its grain boundary. The impedance of such a solid is given by

$$Z^* = A^{*-1} = [1/R_b + jWC_b^*]^{-1} + 1/jWC_{gb}^* \qquad (10)$$

Beside the complex admittance A^*, capacitance C^* and impedance Z^* another complex derivative of permittivity ε^* is still important:

$$c^* = A^*/jWC_0$$
$$= \varepsilon' - j\varepsilon''$$

with C_o is the free space capacitance = ε_o (A/d), ε_o the free space permittivity and A/d the sample geometry of area and thickness.

The real part of permittivity ε' (or **Cb/Co**) corresponds to the dielectric constant and the imaginary part ε'' (or $\varepsilon'\tan\delta$, with $\delta = 90-\theta$) corresponds to the dielectric loss; both are helpful for assigning the mode of conduction and ac-conductivity.

RESULTS AND DISCUSSION

Since the pioneer work of Arrhenius establishing the interdependence of the proton mobility, acidity, conductivity and catalytic activity in zeolites, analysis of the ac-conductivity has been a tool of potential importance in characterization of zeolites. In a previous microcalorimetric study [31], a rise in the acidity has been reported on replacing **B** for **Al** in the alumina structure. Also, **Ga** substitution for **Al** in HZSM-5 reduced the zeolite acidity [32]. These comply with the chemistry of **B, Al** and **Ga.** As expected,incorporation of the less acidic **Ga** for **Al** resulted in losses in HZSM-5 activity. However, it has neither yet been understood nor accepted that replacing the more acidic **B** for **Al** reduces the activity in zeolites. Resolving this confusing conflict has been the subject of a recent ac-conductivity analysis for a progressive substitution of **B** for **Al** in the zeolitic structure of ZSM-5 [26].

In a previous investigation [25] of HZSM-5 conductivity, it has been shown that the real **Z'** and imaginary **Z"** impedances fall with temperature, specially above 373 K, the temperature of boiling water. This is because of the thermally enhanced proton mobility and hence conductivity. Conduction below this temperature is rather assisted by a film of sorbed water that quenches the zeolite grains into tightly gathered aggregates. In essence, the impedance parts are observed to increase with water desorption to maximum at 373 K; above which the role of water is negligible, which is clearly evident in a similar thermodielectic study [33]. Any conductivity rise above 373 K will then be attributed to thermally activated charge carriers, namely the zeolite protons. **TG** and **DTA** analyses of zeolites, particularly of the hydrophobic siliceous type, confirm the entire absence of sorbed water above 423K.

Similar to HZSM-5 [25], the present boralite shows exponential losses in **Z'** and **Z"** (Figs.1a-b) with frequency above 10 kHz. Below this frequency, the impedance parts are less dependent. A correlation analysis shows that boralite conducts with lower impedances than for HZSM-5. Silicalite has incomparably higher impedances in the range 3-5 MOhm at 0.1 kHz even at high temperatures. Analysis of the effect of temperature change on the least frequency dependent **Z'** and **Z"** of boralite reveals a linear trend (Figs.2a-b) diverging at 573 K. The dependence above this temperature is of a higher slope because of a higher conductivity. Such thermal effects can be a consequence of promoted number and/or mobility of the conduction Bronsted sites.

$$\sigma = ne\mu \qquad (11)$$

where n, e and μ are respectively the number, charge and mobility of the conduction charge carriers

HZSM-5, on the other hand, shows a more steady impedance loss with temperature (Figs.2a-b, top plots), probably because of more homogeneously distributed charge carriers. Gamma-irradiation (10 Mrad) of boralite reduces **Z"** (Fig.2b) more than **Z'** (Fig.2a). Irradiation at higher doses, however, raises the impedances (Figs.2a-b) back but to still lower values below those of the fresh sample. Gamma rays appear to participate in the conduction with contrasting effects. While the conduction is assisted at low irradiation doses, the more severe doses show a destructive effect.

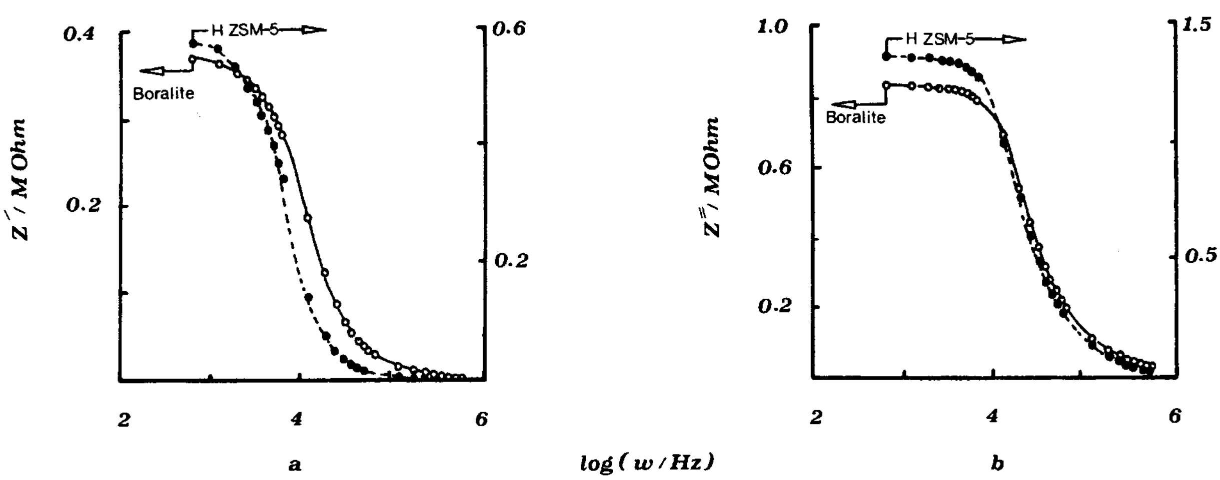

Fig.1 Dependence of the real Z' (a) and imaginary Z" (b) parts of the impedance on frequency W, measured at 658 K for both the boralite and HZSM-5 sieves.

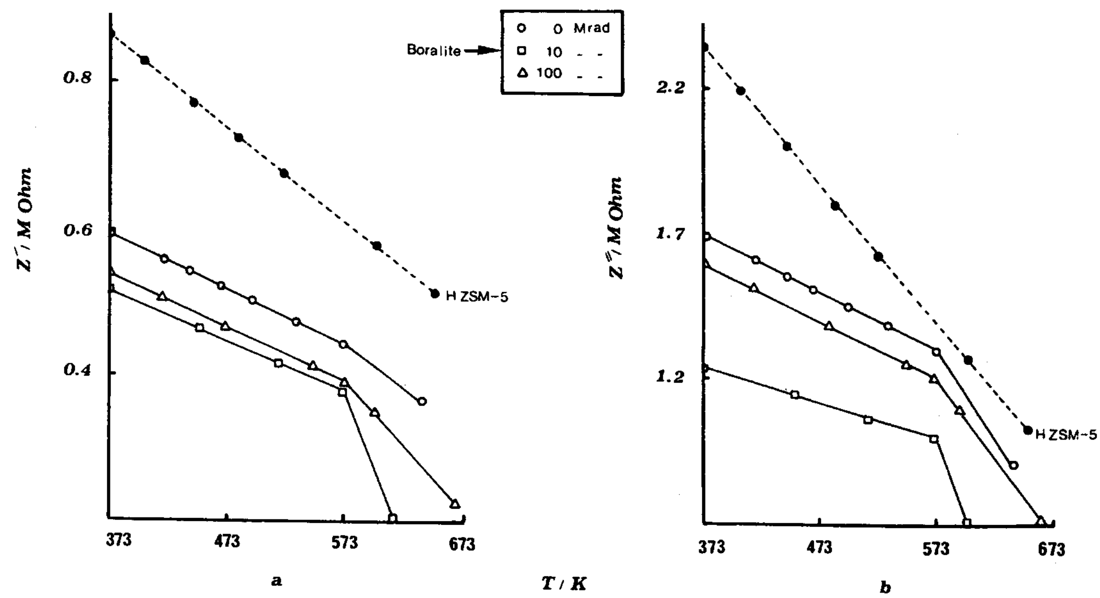

Fig.2 Linear dependence of Z'(a) and Z" (b) on temperature diverging at 573 K for boralite, measured at 0.1 kHz.

As for the impedance, the electric permittivity combines real ε' (a measure of dielectric constant) and imaginary ε" (a measure of dielectric loss) parts. The log dependence of ε' and ε" on frequency **W** (eqn. 12) and the variation with temperature are very important for assigning the conduction mechanism. At 373 K, the dependence shows low frequency dispersion **LFD** of systems conducting via local dipoles that get more polarized on approaching the dc-frequency [34-36]. The **LFD** diminishes with temperatures particularly for ε" as dielectric loss promotes the conduction. Also, low dose (10 Mrad) irradiation induces a farther rise in ε" (Fig.3, top plot) below 10 kHz. Higher dose irradiation (100 Mrad),however,affects boralite controversially where a dramatic drop in ε" prevails. Despite these contrasting effects, ε" drops rather more steadily above 10 kHz. The former rise in ε" below 10 kHz is attributed to polarization of the zeolite protons that may cause dc-conduction, see later. It is also important to admit that while the slope of the logarithmic dependence of eqn. 12 is maintained as nearly unity (**n** approaches zero) below 10 kHz, the higher frequency slope rises with temperature and irradiation because of rising dielectric loss.

$$\varepsilon' \text{ (or } \varepsilon'') \ \alpha \ W^{n-1} \qquad (12)$$

HZSM-5 shows similar **LFD** but at lower permittivities. Silicalite,on the other hand, conducts at considerably lower permittivites and does not show **LFD** that appears to be a characteristic feature of ionic (protonic) conduction.

Fig.4 illustrates the contrasting effects of the irradiation on the boralite conduction. Irradiation below 10 Mrad, while it does not affect the dielectric loss (**tan δ** or ε"/ε' ratio),raises proportionally both the permittivity parts **c'** and **c"**. Irradiation at higher doses reduces the dielectric loss-based conduction. HZSM-5, on the other hand, conducts at lower dielectric losses below those of the 100 Mrad- irradiated boralite sample.

The ac-conductivity δac can be calculated [37] based on the dielectric loss:

$$\sigma_{ac} = \varepsilon_0 \, W \tan \delta \qquad (13)$$

where εo is vacuum permittivity of the cell, W the angular frequency and tan δ the dielectric loss.

Fig.5 shows the effects of varying frequency and temperature on ac-conductivity σ_{ac} Consistent with the impedance loss of Fig.1, σ_{ac} is less dependent on W below 10 kHz and then steeply rises. σ_{ac} also rises with T following two different regimes being discriminated around 500 K (not shown) that also is compatible with Fig.2 showing the shift more precisely at 573 K. Low dose irradiation (10 Mrad) enhances these thermal effects at low frequencies, but has a retarding effect above 10 kHz. σ_{ac} at both the low and high frequency extremes is almost leveled into plateau values due to increased polarization and hence probable contribution of dc-conduction. This appears to associate with the protonic conduction, since silicalite shows no such an effect. Higher dose irradiation (100 Mrad), on the other hand, reduces σ_{ac} in boralite dramatically throughout the frequency range. HZSM-5 conducts at nearly one order lower conductivities but shows steady rise in σ_{ac} at integrated doses. Silicalite shows rather steady conductivity rise with the frequency.

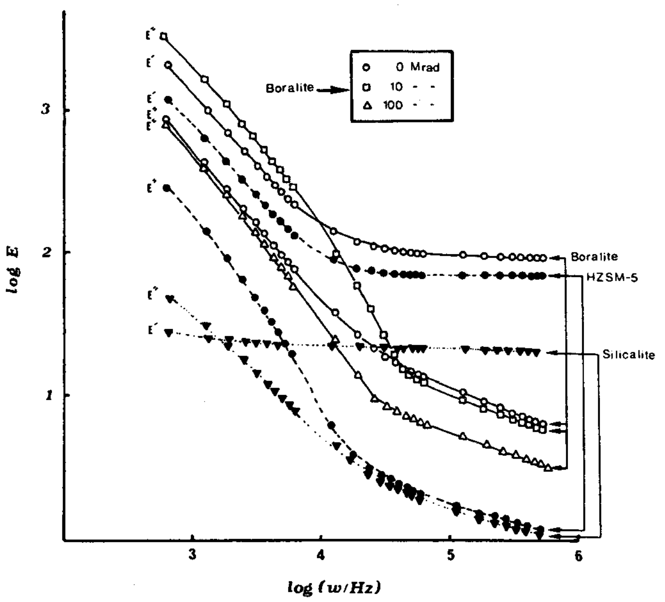

Fig.3 Correlation of the logarithmic dependence of the real ε' and imaginary ε" parts of the permittivity on frequency W for boralite, HZSM-5 and silicalite, measured at 658 K.

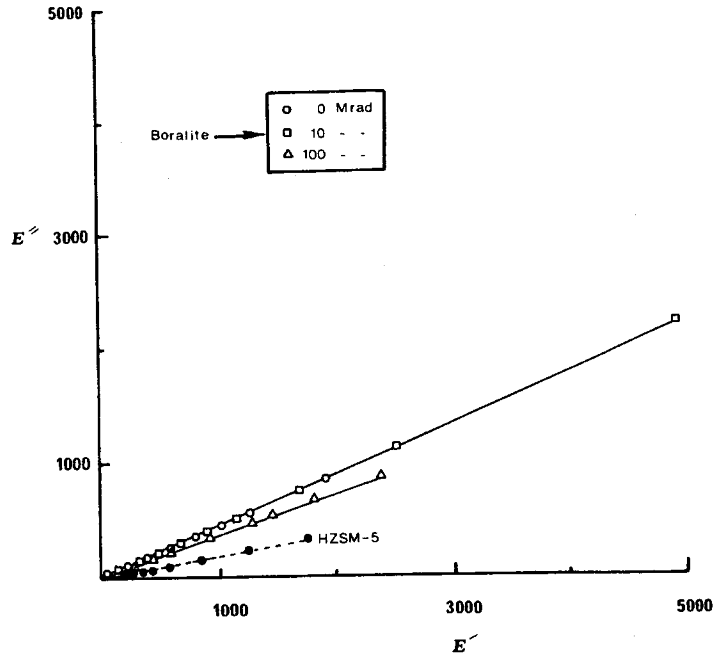

Fig.4 Contrasting effects of gamma-irradiation on the linear ε"(ε') dependence, measured at 658 K.

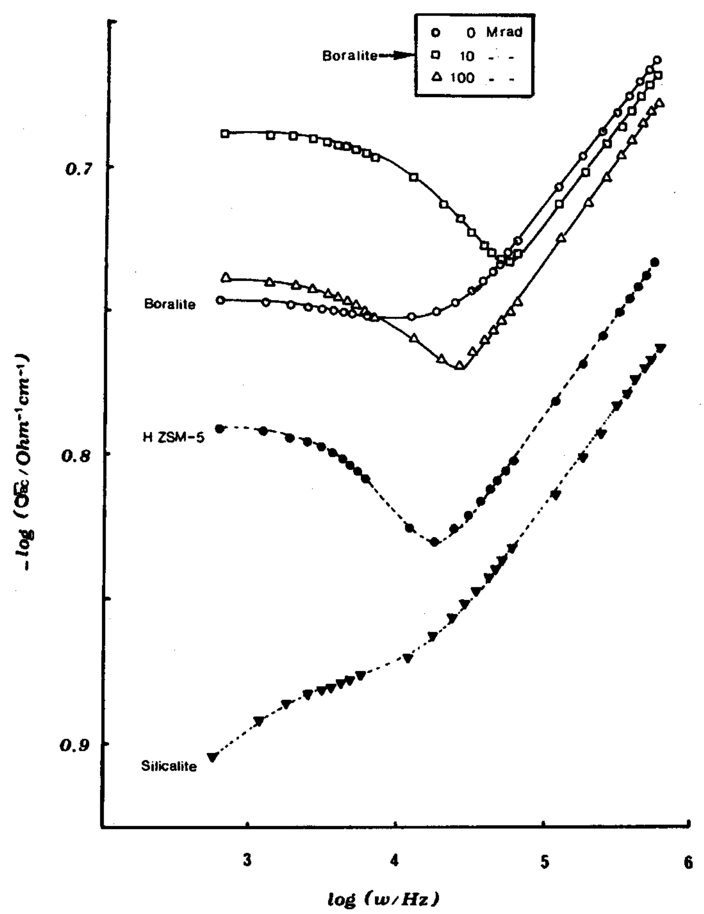

Fig.5 Correlation of the logarithmic dependence of the ac-conductivity on frequency W for boralite, HZSM-5 and silicalite, measured at 658 K.

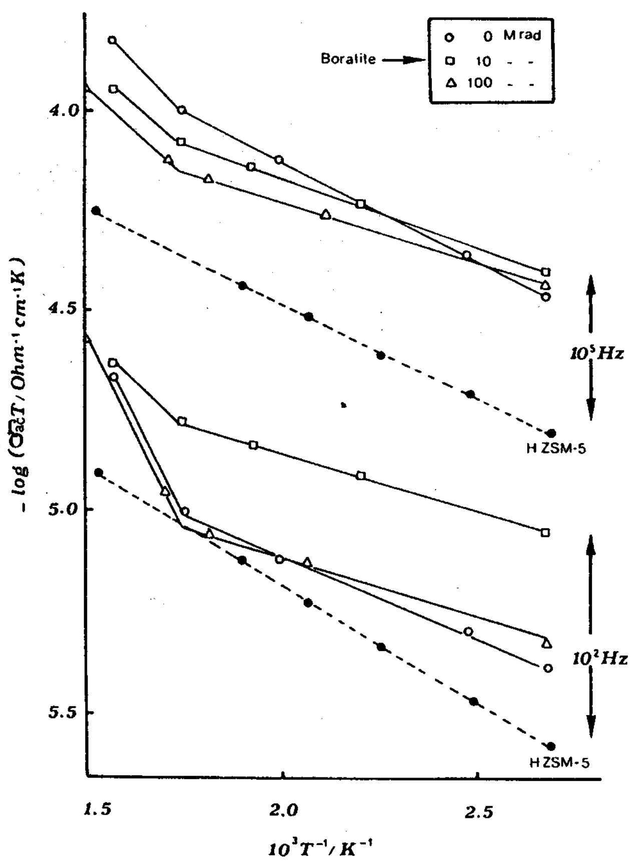

Fig.6 Correlation of the contrasting effects of gamma-irradiation on Arrhenius dependence of log δ T on T^{-1} for boralite, with reference to HZSM-5, measured at 0.1 kHz (bottom plots) and at 100 kHz (top plots).

Now, it appears that the three investigated parameters of the oscillating field frequency,heat temperature and gamma-dose contribute by one way or another to the electric conductivity. They collaborate to affect the conductivity by enhancing the proton mobility. At variance with stable Al-associated Bronsted sites in HZSM-5 [25], B-associated Bronsted sites in boralite are less stable. The latter Bronsted sites exhibit high mobility at low irradiation doses, frequencies and temperatures so that they might not sustain the integrated effects of such parameters. Boralite protons might be trapped in the lattice or be partially dehydroxylated at the more severe treatment conditions [38-41].

Fig.6 illustrates Arrhenius dependence of **log σ_{ac} T on T^{-1}** at varying electric frequencies and irradiation doses.

$$\sigma_{ac} = (A/T)\, e^{-E/kT} \qquad (14)$$

where A is a preexponential constant, E the activation energy and k Boltzmann constant.

Neither the irradiation dose nor the ac-field frequency alters Arrhenius linear dependence that diverges in boralite at 573 K into temperature-controlled regimes of different activation energies. Raising the frequency from 0.10 to 100 kHz raises the activation energy of the low temperature regime slightly from 0.08 to 0.10 eV, but reduces the energy of the high temperature regime significantly from 0.37 to 0.19 eV; i.e. the two regimes merge into a closer energy gap of 0.10-0.19 eV. Also, the low dose (10 M rad) irradiation reduces further the energy into 0.07-0.16 and 0.06-0.13 eV at 0.1 and 100 kHz, respectively. Reduced energy is associated with the increased mobility of B-associated Bronsted sites. Higher dose irradiation raises the energy of the high temperature regime, probably due to rather reduced mobility. This latter result could be due to the trapped protons that might form at severe doses. Reduction in the electric conductivity observed at high irradiation doses and temperatures could then be a result of reduced proton mobility and/or partial dehydroxylation [38-41].The tailing ir band of B-associated Bronsted sites (Fig.7a) in boralite, compared to the more symmetric band (Fig.7b) of Al-associated Bronsted sites in HZSM-5, confirms the presence of heterogeneously distributed B-associated Bronsted sites. The more mobile sites are of low thermal stability.They might under go dehydroxylation at earlier pretreatment stages that would explain the apparently low activity of boralite.

To draw a concise conclusion, discussion of the electric features of boralite should be made with reference to those of a similar history HZSM-5. Boralite shows about one order higher conductivity over HZSM-5 for the fresh samples treated at similar conditions. At variance with the steady rise in conductivity of HZSM-5 with temperature and irradiation (Fig.6 and Ref.25), and despite the higher rise in the borlaite conductivity at low doses and low frequencies, the higher dose irradiation induces major losses in the conductivity of boralite. These contrasting effects can shed light on a probable answer to the low activity of boralite. At variance with homogeneously distributed Al-associated Bronsted sites in HZSM-5, B-associated sites are more heterogeneous. Over the various techniques of catalyst characterization and catalysis that necessarily apply high pretreatment temperatures, this technique of ac-conductivity affords advantageous analysis over a convenient temperature range. The catalytic activity of boralite is highly dependent on both the pretreatment and catalysis temperatures. Low temperatures presume high activity. Higher temperatures inevitably applied in most of the catalyst pretreatments and catalyses preclude the role of the highly mobile B-associated Bronsted sites of low thermal stability and hence renders the boralite sieve apparently inactive!

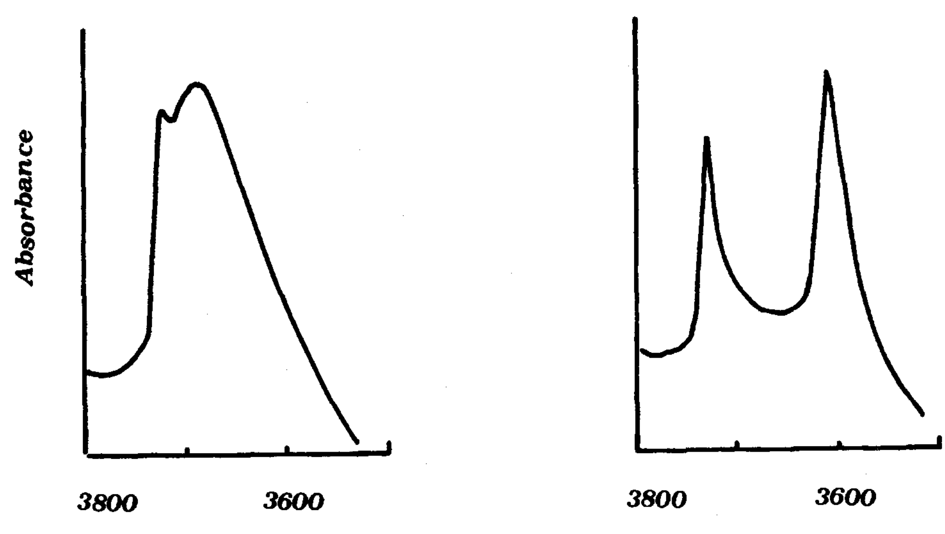

Fig.7 Infrared spectra in the O-H stretching vibrational region of Boralite (a) and HZSM-5 (b), after pretreatment at 10-6 torr and 673 K.

REFERENCES

[1] **Barrer, R.M.** "Hydrothermal Chemistry of Zeolites", Academic Press, (London:1982)

[2] **Taramasso, M. ; G. Perego and B. Notari,** "Proc. of the 5th Int. Conf. on Zeolites, Napoli-1980, Heyden, (London: 1980), p. 40.

[3] **Dessau, R.M. and G.T. Kerr, (1984).** Zeolites, **4**: 315 - 321.

[4] **Chu, C.T.W. and C.D. Chang, (1985).** J. Phys. Chem., **89**, 1569-1573.

[5] **Romanikov, V.M.; L.S. Chumachenko, V.M. Mastikhin and K.G. Ione, (1985).** J. catal., **94**, 508-513.

[6] **Argauer, R.J. and G.R. Landolt, (1972).** U.S. Patent, 3, 702, 886

[7] **Taramasso, M.; G. Manara, V. Fattore and B. Notari, (1980).** French Patent, 2, 429, 182.

[8] **Klotz, R.M., (1981).** U.S. Patents, 4,268,420; 4,285,919 and 4,292,457.

[9] **Kutz, N.A.** "Proc. of the 2nd Symp. of Industry-University Cooperative Chem. Program", Texas A&M Uni. Press, College Station, (Texas: 1984), p. 121.

[10] **Butter, S.A.,** U.S. Patents, 3, 979, 472 (1976) and 4, 007, 231.

[11] **Wu, E.L.; S.L. lawton, D.H. Olson, A.C. Rohrman and G.T. Kokotailo, (1979).** J. Phys. Chem., **83**: 2777-2783.

[12] **Perego, G., M. Cesari and G. Allegra, (1984).** J. Appl. Cryst., **17**, 403-408.

[13] **Meyer, B.L., S.R. Ely, N.A. Kutz and E. Van der Bossche, (1985).** J. Catal., **91**: 352-355.

[14] **Chu, C.T.W., G.H. Kuhel, R.M. Lago and C.D. Chang, (1985).** J. catal., **93**: 451458.

[15] **Gabelica, Z., G. Debra and J.B. Nagy,** in Catalysis on the Energy Scene, Eds. S. Kaliaguine and A. Makay, Stud. Surf. Sci. Catal. Series, Vol. 23 Elsevier, (Amsterdam: 1984), p. 113.

[16] **Holderich, N.; H. Eichon, R. Lehnert, L. Marosi, W. Mross, R. Reinke, W. Ruppel and H. Schlimper,** "Proc. of the 6th Int. Conf. on Zeolites, (Reno-1983), Eds. D. Olson and A. Bisio, Butterworth, (London: 1984), p. 545.

[17] **Board, R.B.; A.B. Halgeri and T.S.R. Prasad Rao,** "Proc. of the 7th Int. Conf. on Zeolites, Eds. Y. Murakami, A. Lijima and J.W. Ward, Elsevier, (Amsterdam:1986) p. 581.

[18] **Beyer, M.K. and G. Borberly,** "Proc. of the 7th Int. Conf. on Zeolites, Eds. Y. Murakami, A. Lijima and J.W. Ward, Elsevier, (Amsterdam: 1986) 867.

[19] **Scholle, K.F.M.G.J.; A.P.M. Kentgens, W.S. Veeman, P. Frenken and G.P.M. Van der Velden, (1984).** J. Phys. Chem., **88:** 5.

[20] **Nieto, M.I.; A. Duran, J.M.F. Navarro and J.L.O. Nazo, (1984).** J. Amer. Ceramic Soc., **67**: 242-246.

[21] **Coudurier, G. and J.C. Vedrine, (1986).** Pure Appl. Chem., **58**: 1389-1398.

[22] **Sayed, M.B., A. Auroux and J.C. Vedrine, (1989).** J. Catal., **116:**, 1 -10.

[23] **Auroux, A., G. Coudurier, R. Shannon and J.C. Vedrine, (1985).** "Proc. APCAT Meeting, Montpellier-1985, Eds. S. Patryka and M. Lidheimer, **16**: 68-76.

[24] **Sayed, M.B., (1988).** Thermochim. Acta, **126**: 325-337.

[25] **Sayed, M. B., A. A. Higazy and M.E. Kassem, (1992).** J. Phys. Chem. Solids, **53/4**: 549-554.

[26] **Sayed, M.B. (1996).** Microporous Materials, **6(4):** 181-188.

[27] **Guth, J.L.; H. Kessler, M. Bourgogne and R. Wey,** French Patent, 85-07978.

[28] **Guth, J.L.; H. Kessler and R. Wey,** "Proc. of the 7th Int. Conf. on Zeolites", Eds. Y. Murakami, A. Lijima and J.W. Ward, Elsevier, (Amsterdam: 1986).

[29] **Coudurier, G.; C. Naccache and J.C. Vedrine, (1982).** JCS, Chem. Commun., 1413-1416.

[30] **Mentzen, B.F. and J.C. Vedrine, C. R. Paris, (1985).** 301 ser.II, 1017.

[31]. **Colorio, G.C.; A. Auroux and B. Bonnetat, (1993).** J. Thermal Anal., **40**: 1267-1276.

[32] **Awate, S.V.; P.N. Joshi, M.J. Eapen and V.P. Shiralkar, (1993).** J. Phys. Chem., **97**: 6042-6047.

[33] **Malehrb R.R. and A. Montes, (1986).** J. Thermal Anal., **31**: 517-521.

[34] **Jonscher, A.K.** "Universal Relaxation Law", Chelsea Dielectrics Press, (London: 1991).

[35] **Jonscher, A.K.** "Dielectric Relaxation in Solids", Chelsea Dielectrics Press, (London: 1983).

[36]. **Nikelsson, G.A., (1987).** "Fractal Aspects of the Dielectric Response of Charge Carriers in Disordered Materials", J. Applied Phys., **62**: R1.

[37] **Sirdeshmukh, L., G. Sathala and P. Devi, (1987).** Phys. State Sol., **99:** 631-639.

[38] **Abu-Kais, A.; J.C. Vedrine, J. Massardier and B. Dalmi Imelik, (1974).** J. catal., **34**: 317.

[39] **Dikanov, S.A.; R.I. Samoilov and Y.D. Tsretkov, (1979).** J. Phys. Chem., **83**: 2515-2519.

[40] **Sayed, M.B. (1992).** J. Phys. Chem. Solids, **53/8**: 1041-1048.

[41] **Sayed, M.B. (1993).** Thermochim. Acta, **219**: 73-82.

Received 1 May, 1996